Colloid and Interface Science Communications 40 (2021) 100342

Contents lists available at ScienceDirect

Colloid and Interface Science Communications

journal homepage: www.elsevier.com/locate/colcom

Unexpected observation of an intermediate hexagonal phase upon fluid-to-gel transition: *SDS self-assembly in glycerol*

Lauren Matthews [a,b,1], Michael C. Stevens [a], Ralf Schweins [c], Paul Bartlett [a], Andrew J. Johnson [d], Robert Sochon [d], Wuge H. Briscoe [a,*]

[a] School of Chemistry, University of Bristol, Cantock's Close, Bristol BS8 1TS, UK
[b] Bristol Centre for Functional Nanomaterials, HH Wills Physics Laboratory, University of Bristol, Tyndall Avenue, Bristol BS8 1TL, UK
[c] Institut Laue-Langevin, DS/LSS, 71 Avenue des Martyrs, Grenoble 38000, France
[d] GlaxoSmithKline, St George's Avenue, Weybridge KT13 0DE, UK

ARTICLE INFO

Keywords:
Glycerol
SDS
Surfactant mesophases
Nonaqueous H-bonding solvents
Small-angle neutron scattering
Self-assembly
Gelation
Low molecular-weight gels
Lamellar phase
Hexagonal phase

ABSTRACT

Understanding morphological transformations upon temperature-induced mesophase transitions offers mechanistic insights into the self-assembly process. We have recently reported the unexpected formation of a microfibrillar lamellar gel in SDS-glycerol mixtures above a critical gelation concentration (CGC) as low as ~2 wt%. The gel phase comprised a fibrillar structure on the microscale and a lamellar structure on the nanoscale. Here, the nanoscopic structure of the gel as a function of temperature was probed with small-angle neutron scattering (SANS). The gel underwent a gel-to-fluid transition at a critical gelation temperature, T_{GC} = 45 °C, forming cylindrical micelles at elevated temperatures. Upon cooling, a hexagonal phase formed at ~T_{GC}, evident from the SANS Bragg peaks. This hexagonal phase upon the fluid-to-gel transition sheds light on the gelation mechanism, in which self-assembled SDS micelles undergo a cylindrical-to-lamellar morphological transition *via* a hexagonal phase. This unprecedented observation also highlights the complexity of self-assembly in nonaqueous hydrogen-bonding rich media.

1. Introduction

Understanding the mechanism of thermotropic mesophase transitions is important to many applications, ranging from industrial formulations to biological processes. For instance, it is relevant to the molecular mechanisms of endocytosis [1] and cryobiology [2], as well as polymorphs of chocolate [3–6] and soaps [7–10] at elevated temperatures during their formulation processes.

The lamellar-to-hexagonal lipid mesophase transition has been widely studied due to its relevance to the molecular deformations involved in the membrane fusion process, in which non-bilayer intermediates could form as postulated in the Stalk model [11]. In particular, phosphatidylethanolamine (PE) lipids are reported to be prone to the formation of the hexagonal phase in physiological conditions, and are thus implicated in mediating membrane fusion [12,13]. For instance, the kinetics of the reversible lamellar-to-inverse hexagonal phase transition of dihexadecyl phosphatidylethanolamine (DHPE) has been previously probed with X-ray diffraction (XRD), suggesting that the temperature-induced shift in the free energy of the lipid molecule caused its molecular shape to change from a wedge to a rod upon the transition [14–17]. It has also been reported that the tetraoleoyl cardiolipin lamellar phase formed a hexagonal phase in the presence of 3.5 M sodium chloride (NaCl) [18].

Using XRD, Yang and Huang demonstrated the formation of an intermediate 'stalk' (an hourglass shape) phase upon fusion of lipid bilayers [19]. The formation of this intermediate phase was predicted mathematically [20], where the energy of the structure was determined by the lipid chain splay and tilt, which is dependent on the membrane composition [21–23]. The formation of the stalk intermediate has also been observed in self-assembled structures of lung surfactant in the presence of a hydrophobic protein (SP-B) [24], conjectured to be relevant to fatal neonatal respiratory diseases due to SP-B deficiency [25].

Temperature-induced phase transitions are common in surfactant systems. For instance, the isotropic to hexagonal phase transition in Triton X100 aqueous media occurs at T = 33 °C [26,27]. A transition from the lamellar gel phase to micellar and lamellar liquid crystalline

* Corresponding author.
E-mail address: wuge.briscoe@bristol.ac.uk (W.H. Briscoe).
[1] Current address: The European Synchrotron Radiation Facility, 38043 Grenoble, France.

https://doi.org/10.1016/j.colcom.2020.100342
Received 11 October 2020; Received in revised form 12 November 2020; Accepted 15 November 2020

phases was observed in aqueous solution of anionic sodium lauryl sulfoacetate at $T > 50$ °C [28]. Lysine-based surfactants were reported to undergo a phase transition from micellar aggregates to a gel phase upon cooling below its Krafft temperature due to its suppressed solubility [29].

Molecular dynamic (MD) simulations of sodium dodecyl sulfate (SDS) in aqueous salt solutions (700 mM calcium chloride, $CaCl_2$) showed micelle fission *via* a stalk intermediate [30], similar to that in the lipid membrane fusion process. However, experimental observations of intermediate structures upon surfactant mesophase transitions have not been reported.

Here, we report that an intermediate hexagonal phase formed in the fluid-to-gel transition upon cooling of 4.4 wt% sodium dodecyl sulfate (SDS)-in-glycerol gel. The supramolecular gel was thermally reversible [31], and below a critical gelation temperature (T_{CG}) ~ 45 °C, the gel phase comprised a fibrillar structure on the microscale and a lamellar structure on the nanoscale. Above T_{CG}, the fluid phase consisted of cylindrical SDS micelles. Intriguingly, upon cooling from the fluid phase, an intermediate hexagonal phase formed, which has not been previously reported, including in aqueous SDS systems [32,33]. The nanostructures of the fluid-, intermediate-, and gel-phase were probed using small-angle neutron scattering (SANS). The observation of this intermediate phase highlights the complexity of self-assembly in H-bonding non-aqueous media, which is very different from the aqueous medium. Although our focus here is the mesophase phase transition, we note that hydrogels and nanocomposite gels with different intricate nanostructures that are tuneable by external conditions have potential in a wide range of applications (*e.g.* [34,35]). Thus, understanding the mechanism of the gelation mechanism in our novel nonaqueous lamellar gels is important to their potential future applications.

2. Materials and methods

2.1. Materials

h-Sodium dodecyl sulfate (SDS) (Sigma-Aldrich, >98.0%) was recrystallised three times from ethanol prior to use, and its purity was checked with ^{1}H NMR. *h*-Glycerol (Fisher Scientific, >98.0%) and d-Glycerol (Sigma-Aldrich, >98.0% and >98.0 atom % D) were used as received. All glycerol-containing (both *hydrogenated* (*h*-) and *deuterated* (d-)) phases and controls were kept sealed from moisture. The gel-like phase was prepared by adding *h*-SDS to *h*- or d-glycerol, then incubating and shaking (at 550 RPM) the mixture in a shaker incubator (Stuart SI505) for two hours (2 h) at 60 °C, before equilibrating at room temperature overnight.

2.2. Polarised light microscopy (PLM)

PLM was carried out using an Olympus BX53-P microscope, where the polarisers were crossed at 90° with respect to each other and images were captured using Stream software. PLM measurements were carried out under ambient conditions, using 10, 20, and 40 × magnifications. A 530 nm first order waveplate was placed into the optical path to enhance image contrast.

2.3. Small-angle neutron scattering (SANS)

SANS data was obtained from samples contained in quartz cells with a 2 mm path length on the D11 [36,37] small-angle diffractometer at the Institut Laue-Langevin, ILL, (Grenoble, France). A neutron beam with wavelength (λ = 5.5 Å with a FWHM of 9%) and three sample-to-detector distances (1.4, 8, and 39 m) were used to obtain a q-range of ~0.0016–0.5 Å^{-1}, where $q = 4\pi \sin(2\theta/2)/\lambda$ is the momentum transfer with 2θ the scattering angle. The raw scattering data was corrected for the detector efficiency, sample transmission, and background scattering and converted to scattering cross-section data ($\partial\Sigma/\partial\Omega$ *vs* q) using LAMP. The data was converted to an absolute scale (cm^{-1}) using the secondary calibration standard H_2O of 1 mm path length (cross-calibrated against h/d polymer blends sample) with a differential scattering cross section of 0.956 cm^{-1}.

2.4. SANS data analysis

The Bragg peaks obtained in the raw scattering profiles were fitted with Gaussian functions using Igor Pro to determine the peak positions (q), the peak full width-half maximum (Δq), and the coherence length (L_c) of the mesophase. The ratio of the peak positions was used to ascertain the surfactant mesophases present in the samples, and the lamellar d-spacing was also taken from the peak position,

$$d = \frac{2\pi}{\boldsymbol{q}} \quad (1)$$

The coherence length L_c, indicative of the structural order in the mesophase, was calculated using the Scherrer equation [38–45]

$$L_c = \frac{2\pi K}{\Delta \boldsymbol{q}} \quad (2)$$

where K is a shape factor of order unity.

3. Results and discussion

In a previous paper [31], we have reported the formation of a thermally reversible SDS-in-glycerol lamellar gel above a critical SDS gelation concentration (c_{CGC} ~ 2 wt%) and below a critical gelation temperature (T_{GC} ~ 45 °C; Curve 1 and 4, Fig. 1a). The gel phase consisted of entangled fibres comprising SDS lamellar micro-domains at room temperature, which transformed into *cylindrical micelles* above T_{GC} (Curve 2, Fig. 1a). The lamellar Bragg peaks noted, previously and here, have a corresponding d-spacing, d = 5.7 nm. Here, we focus on the self-assembled intermediate structure upon the fluid-to-gel transition. For 4.4 wt% SDS in glycerol, an additional Bragg peak appeared after cooling to 25 °C at q ~ 0.197 Å^{-1} (indicated by an arrow on Curve 3, Fig. 2; *cf.* Table 1), which was not observed before heating (Curve 1, Fig. 2). With respect to the first Bragg peak position q_0 ~ 0.1 Å^{-1}, this peak was at ~ $\sqrt{3}\boldsymbol{q}_0$, indicative of a hexagonal phase for which the Bragg peak ratio would be 1, $\sqrt{3}$, $\sqrt{4}$ … [46]. This suggests that, upon cooling, the cylindrical micelles observed in the fluid phase above T_{GC} condensed into an intermediate hexagonal phase before transforming into the lamellar phase at thermodynamic equilibrium. We note that the cooling process took place *in situ* at the SANS beamline over ~30 min at a rate of ~1.5 °C min^{-1}, with a waiting time of 4 h before the measurement, which appeared insufficient to reach the equilibrium structure, probably due to the high viscosity of the hexagonal phase. For comparison, in a previous measurement at ISIS Loq beamline, we observed the equilibrium structure after ~8 h cooling (Curve 4 in Fig. 1) using a similar cooling rate as that at ILL.

The SANS results have confirmed the formation of an intermediate phase in the fluid-to-gel transition upon cooling of the SDS-in-glycerol system. The SANS profile before heating and after overnight (~8 h) cooling were identical, suggesting the thermodynamic equilibrium structure was the lamellar gel phase noted previously [31]. The hexagonal intermediate phase has not been previously reported, whilst the phase diagram of SDS in aqueous media shows that a lamellar-to-hexagonal transition would occur upon cooling [32,33] but at a much higher c_{SDS} ~ 80 wt%. At c_{SDS} = 4.4 wt% in water, a micellar phase of spherical or ellipsoidal shape exists [47–49], with no temperature-induced phase transition, in contrast to the behaviour observed here in glycerol. This points to the drastically different self-assembly driving forces in water and in glycerol, despite their similar physical properties such as H-bonding capacity and both being polar, as discussed in Ref. [31].

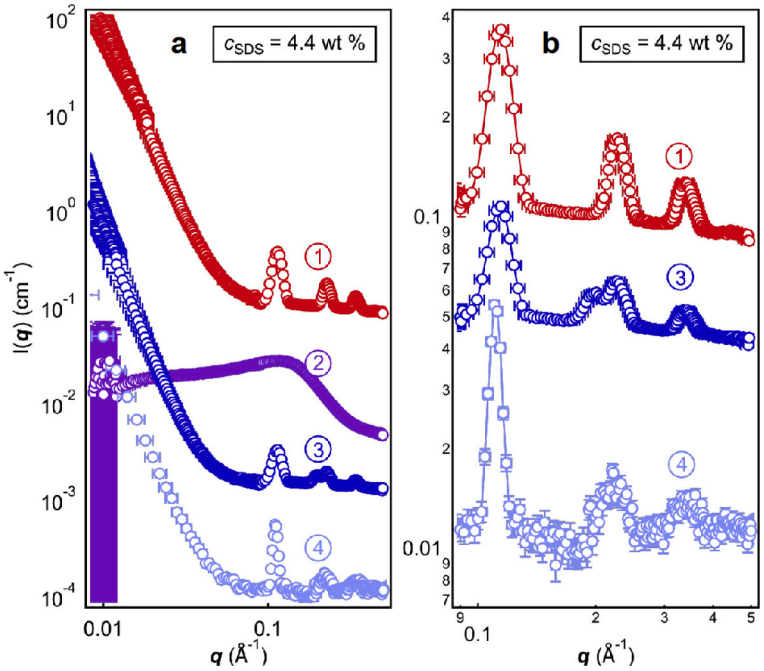

Fig. 1. (a) SANS profiles of 4.4 wt% SDS in glycerol at 25 °C before heating (**red**, **1**), at 70 °C (**purple**, **2**), 25 °C after cooling for ~4 h (**blue**, **3**), and 25 °C after cooling for ~8 h (**light blue**, **4**). The SANS profile at 70 °C could be fitted to a cylinder model (*cf.* Fig. 3) with a radius of $r = 1.7$ nm and or length$l = 1.2$ nm, discussed in detail [31]. (b) The gel phase scattering profiles zoomed in around the Bragg peaks. The data for **4** (**light blue**) was obtained at the ISIS Loq beamline included for comparison [31], and the data for all the other profiles were obtained at the ILL D11 beamline. The SANS profiles are offset for clarity (**Curve**, shift factor: **1**, 1; **2**, 0.1; **3**, 0.01; **4**, 0.01). (For interpretation of the references to colour in this figure legend, the reader is referred to the web version of this article.)

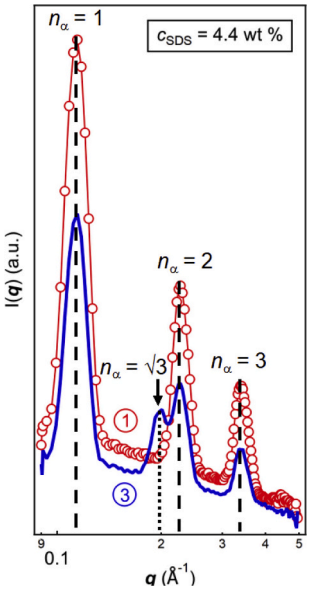

Fig. 2. Overlaid SANS profiles of 4.4 wt% SDS in glycerol at 25 °C before heating (**red**, **1**), and 25 °C after cooling for ~4 h (**blue**, **3**), zoomed in around the Bragg peaks. The numbering of the curves is the same as that in Fig. 1. (For interpretation of the references to colour in this figure legend, the reader is referred to the web version of this article.)

Table 1
Bragg peak positions in q (Å^{-1}) and peak ratio obtained from the SANS profiles of the SDS-in-glycerol gel (c_{SDS} = 4.4 wt%) at different temperatures, T. Also listed are the d-spacing ($d_{lamellar}$, for the lamellar phase) and the correponding mesophase.

T (°C)	Peak q-Position (Å^{-1})	Peak Ratio	$d_{lamellar}$ (Å)	Phase
25[a]	0.114 ± 0.001	1	–	Lamellar
	0.228 ± 0.002	2	55.3	
	0.340 ± 0.002	3	55.6	
25[b]	0.114 ± 0.003	1	–	Lamellar +
	0.197 ± 0.004	√3	–	Hexagonal
	0.227 ± 0.003	2	55.3	
	0.340 ± 0.003	3	55.8	
25[c]	0.114 ± 0.003	1	–	Lamellar +
	0.197 ± 0.007	√3	–	Hexagonal
	0.228 ± 0.005	2	55.2	
	0.341 ± 0.003	3	55.6	
	0.111 ± 0.001	1	–	Lamellar
25[d]	0.223 ± 0.001	2	56.1	
	0.342 ± 0.002	3	52.8	

Sample data before heating at 25 °C[a] and after cooling to 25 °C for 2 h[b], 4 h[c], and 8 h[d] respectively.

The formation of intermediate phases adds further details to the proposed mechanism for the gelation of SDS in glycerol at low concentrations – itself an unprecedented observation [31]. Here we have observed that the fluid phase consisting of cylindrical micelles cools *via* a hexagonal phase before forming the lamellar phase at thermodynamic equilibrium. The fluid-to-gel phase transition can be considered as two steps (Fig. 3): the formation of the hexagonal phase from condensation or packing of the cylindrical micelles, and fusion of the hexagonal phase to form the lamellar phase. The first step is driven by the reduction in the kinetic energy and rigidification of the self-assembled objects and the increase in the solvent viscosity upon cooling. Entropically, this would allow for the formation of a more ordered phase to retain a favourable free energy. The increase in the solvent viscosity would also reduce the ability of micellar aggregates to diffuse through the solvent in bulk, allowing for the intermediate hexagonal phase to be observed.

The second step in the fluid-to-gel transition comprises the hexagonal-to-lamellar transition, where the molecular shape transforms from wedge to rod, noted by Caffrey [14], based on the packing parameter [50,51]. The metastable hexagonal phase is kinetically stabilised due to the preference of SDS molecular packing in a conical-wedge molecular shape, as per aqueous solutions with a packing parameter ~0.3. The tail volume tends to decrease with increasing temperature, a result of the increased kinetic energy allowing for optimal tail conformation, and, thus the opposite holds true upon cooling [52]. The decreasing temperature can thus account for an increase in the tail volume, leading to an increase in the packing parameter, explaining why the structure at thermodynamic equilibrium returns to the lamellar morphology. Another subtle contribution could

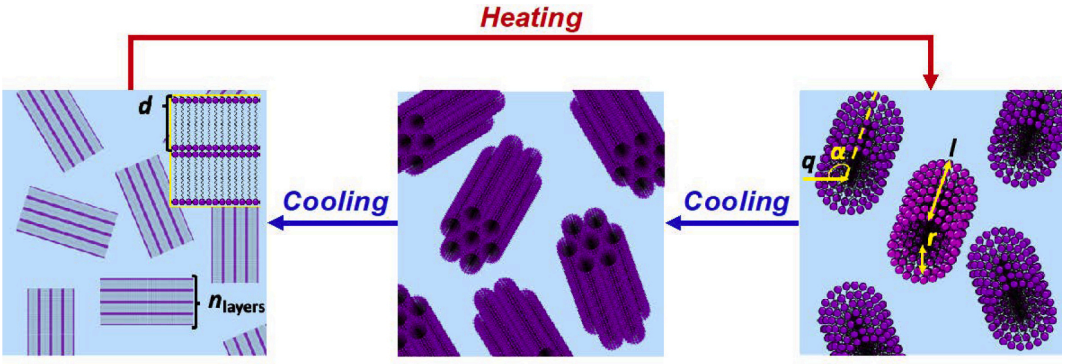

Fig. 3. A schematic representation of the gel-to-fluid transition at elevated temperatures, and the fluid-to-gel transition *via* the hexagonal intermediate with upon cooling.

derive from the slightly reduced solubility of Na^+ counterions at the lower temperature. Initial cooling would drive more Na^+ to condense on the micelle surface, screening charge repulsion between the headgroups and allowing micelle condensation into the 2D hexagonal phase. Further slow diffusion of Na^+ and condensation on the micelle surface would further shrink the headgroup size. Along with the increased tail volume at the lower *T* (as discussed above), this would further increase the effective packing parameter, until the lamellar phase is favoured.

Our results here, in combination with our previous observation of the SDS-in-glycerol gel [31], have shown that the gelation mechanism of surfactants in polar-nonaqueous media is more complex than previously thought. Our previous results of SDS in glycerol showed a microfibrillar gel phase with lamellar nanostructure [31] at room temperature, transitioning to a fluid phase consisting of cylindrical aggregates interacting *via* a Coulombic pair potential. However, here we report the presence of a metastable intermediate phase (Fig. 3), which is kinetically stable as a result of decreasing entropy and increasing bulk viscosity. It is an important consideration in the gelation mechanism, offering insights to further elucidate the self-assembly mechanism of surfactants in nonaqueous H-bonding rich media. This mechanistic understanding has important implications in a variety of applications, for instance in formulations where viscous polar-nonaqueous media are prevalent.

Author contributions

L.M. and W.H.B. designed experiments and secured neutron beam time.

L.M., M.C.S., R.S., and WHB conducted SANS experiments.

L.M. and W.H.B. analysed the SANS data.

R.S., A.J.J., P.B., and W.H.B. supervised L.M.

L.M. wrote the first draft of the manuscript and then co-wrote the subsequent versions of the manuscript with W.H.B., with all the other co-authors contributing to the editing and reviewing of the final draft of the manuscript.

Declaration of Competing Interest

The authors declare that they have no known competing financial interests or personal relationships that could have appeared to influence the work reported in this paper.

Acknowledgements

We acknowledge the Institut Laue-Langevin for the awarded beamtime under experiment number: 9-10-1586 [DOI https://doi.org/10.5291/ILL-DATA.9-10-1586]. We acknowledge ISIS Muon and Neutron source for the awarded beamtime under experiment number: 1810629. L.M. was supported by a joint studentship through the Bristol Centre for Functional Nanomaterials (Engineering and Physical Science Research Council (EPSRC) EP/L016648/1) and GlaxoSmithKline, and M.C.S. by a joint studentship through Infineum and EPSRC Doctoral Training Partnership Industrial and International Leverage Fund.

References

[1] L. Cruzeiro-Hansson, J.H. Ipsen, O.G. Mouritsen, Biochim. Biophys. Acta Biomembr. 979 (1989) 166–176.
[2] P.J. Quinn, Cryobiology 22 (1985) 128–146.
[3] J. Bricknell, R.W. Hartel, J. Am. Oil Chem. Soc. 75 (1998) 1609–1615.
[4] D.J. Cebula, G. Ziegleder, Lipid/Fett 95 (1993) 340–343.
[5] G. Mazzanti, S.E. Guthrie, E.B. Sirota, A.G. Marangoni, S.H.J. Idziak, Cryst. Growth Des. 3 (2003) 721–725.
[6] S. Sonwai, D. Rousseau, Food Chem. 119 (2010) 286–297.
[7] D.P. Cistola, D. Atkinson, J.A. Hamilton, D.M. Small, Biochemistry 25 (1986) 2804–2812.
[8] M.N.G. de Mul, H.T. Davis, D.F. Evans, A.V. Bhave, J.R. Wagner, Langmuir 16 (2000) 8276–8284.
[9] H.J. Merle, R. Steitz, U. Pietsch, I.R. Peterson, Thin Solid Films 237 (1994) 236–243.
[10] S. Zhu, M. Heppenstall-Butler, M.F. Butler, P.D.A. Pudney, D. Ferdinando, K. J. Mutch, J. Phys. Chem. B 109 (2005) 11753–11761.
[11] D. Marsh, Chem. Phys. Lipids 57 (1991) 109–120.
[12] J. Boggs, D. Stamp, D. Hughes, C. Deber, Biochemistry 20 (1981) 5728–5735.
[13] K. Gawrisch, V.A. Parsegian, D.A. Hajduk, M.W. Tate, S.M. Gruner, N.L. Fuller, R. P. Rand, Biochemistry 31 (1992) 2856–2864.
[14] M. Caffrey, Biochemistry 24 (1985) 4826–4844.
[15] J.M. Seddon, G. Cevc, R.D. Kaye, D. Marsh, Biochemistry 23 (1984) 2634–2644.
[16] J.M. Seddon, R.H. Templer, Philosophical Trans. Phys. Sci. Eng. 344 (1993) 377–401.
[17] M. Rappolt, A. Hickel, F. Bringezu, K. Lohner, Biophys. J. 84 (2003) 3111–3122.
[18] M.B. Sankaram, G.L. Powell, D. Marsh, Biochim. Biophys. Acta Biomembr. 980 (1989) 389–392.
[19] L. Yang, H.W. Huang, Science 297 (2002) 1877.
[20] V.S. Markin, M.M. Kozlov, V.L. Borovjagin, Gen. Physiol. Biophys. 3 (1984) 361–377.
[21] Y. Kozlovsky, M.M. Kozlov, Biophys. J. 82 (2002) 882–895.
[22] V.S. Markin, J.P. Albanesi, Biophys. J. 82 (2002) 693–712.
[23] D.P. Siegel, Biophys. J. 76 (1999) 291–313.
[24] S. Baoukina, D.P. Tieleman, Biophys. J. 100 (2011) 1678–1687.
[25] L.M. Nogee, G. Garnier, H.C. Dietz, L. Singer, A.M. Murphy, D.E. deMello, H. R. Colten, J. Clin. Invest. 93 (1994) 1860–1863.
[26] S.V. Ahir, P.G. Petrov, E.M. Terentjev, Langmuir 18 (2002) 9140–9148.
[27] K. Beyer, J. Colloid Interface Sci. 86 (1982) 73–89.
[28] A. Bhadani, A. Kafle, T. Ogura, M. Akamatsu, K. Sakai, H. Sakai, M. Abe, Ind. Eng. Chem. Res. 58 (2019) 6235–6242.
[29] I.S. Oliveira, M. Lo, M.J. Araújo, E.F. Marques, Soft Matter 15 (2019) 3700–3711.
[30] M. Sammalkorpi, M. Karttunen, M. Haataja, J. Am. Chem. Soc. 130 (2008) 17977–17980.
[31] L. Matthews, Ż. Przybyłowicz, S.E. Rogers, P. Bartlett, A.J. Johnson, R. Sochon, W. H. Briscoe, J. Colloid Interface Sci. 572 (2020) 384–395.
[32] P. Kekicheff, J. Colloid Interface Sci. 131 (1989) 133–152.
[33] P. Kekicheff, C. Grabiellemadelmont, M. Ollivon, J. Colloid Interface Sci. 131 (1989) 112–132.
[34] T. Jiao, H. Zhao, J. Zhou, Q. Zhang, X. Luo, J. Hu, Q. Peng, X. Yan, ACS Sustain. Chem. Eng. 3 (2015) 3130–3139.
[35] J. Song, C. Yuan, T. Jiao, R. Xing, M. Yang, D.J. Adams, X. Yan, Small 16 (2020), e1907309.
[36] K. Lieutenant, P. Lindner, R. Gahler, J. Appl. Crystallogr. 40 (2007) 1056–1063.
[37] L. Matthews, M. Stevens, R. Schweins, W.H. Briscoe, et al., Molecular self-assembly in hydrogen-bonding rich non-aqueous solvents, Institut Laue-Langevin (ILL) (2019), https://doi.org/10.5291/ILL-DATA.9-10-1586.

[38] C.M. Beddoes, J. Berge, J.E. Bartenstein, K. Lange, A.J. Smith, R.K. Heenan, W. H. Briscoe, Soft Matter 12 (2016) 6049–6057.
[39] J.M. Bulpett, A.M. Collins, N.H.M. Kaus, P.T. Cresswell, O. Bikondoa, D. Walsh, S. Mann, S.A. Davis, W.H. Briscoe, J. Mater. Chem. 22 (2012) 15635–15643.
[40] J.M. Bulpett, T. Snow, B. Quignon, C.M. Beddoes, T.Y.D. Tang, S. Mann, O. Shebanova, C.L. Pizzey, N.J. Terrill, S.A. Davis, W.H. Briscoe, Soft Matter 11 (2015) 8789–8800.
[41] T.G. Dane, J.E. Bartenstein, B. Sironi, B.M. Mills, O. Alexander Bell, J. Emyr Macdonald, T. Arnold, C.F.J. Faul, W.H. Briscoe, Phys. Chem. Chem. Phys. 18 (2016) 24498–24505.
[42] T.G. Dane, P.T. Cresswell, G.A. Pilkington, S. Lilliu, J.E. Macdonald, S.W. Prescott, O. Bikondoa, C.F.J. Faul, W.H. Briscoe, Soft Matter 9 (2013) 10501–10511.
[43] L.J. Fox, L. Matthews, H. Stockdale, S. Pichai, T. Snow, R.M. Richardson, W. H. Briscoe, Acta Biomater. 104 (2020) 198–209.
[44] N.H.M. Kaus, A.M. Collins, O. Bikondoa, P.T. Cresswell, J.M. Bulpett, W.H. Briscoe, S. Mann, J. Mater. Chem. C 2 (2014) 5447–5452.
[45] B. Sironi, T. Snow, C. Redeker, A. Slastanova, O. Bikondoa, T. Arnold, J. Klein, W. H. Briscoe, Soft Matter 12 (2016) 3877–3887.
[46] C.V. Kulkarni, W. Wachter, G. Iglesias-Salto, S. Engelskirchen, S. Ahualli, Phys. Chem. Chem. Phys. 13 (2011) 3004–3021.
[47] G.B. Ray, I. Chakraborty, S. Ghosh, S.P. Moulik, Colloid Polym. Sci. 285 (2007) 457–469.
[48] C. Tanford, J. Phys. Chem. 76 (1972) 3020–3024.
[49] C. Tanford, The Hydrophobic Effect: Formation of Micelles and Biological Membranes, 2nd edn., Wiley & Sons, New York, US, 1976.
[50] J. Israelachvili, Colloid. Surf. 91 (1994) 1–8.
[51] J.N. Israelachvili, Intermolecular and Surface Forces, Academic press, 2011.
[52] T.L. Lin, M.Y. Tseng, S.H. Chen, M.F. Roberts, J. Phys. Chem. US 94 (1990) 7239–7243.